

Examining the respiratory activity of Chinese Hamster Ovary (CHO) cell pool expressing SARS-CoV-2 spike protein across shake flask scales using the Transfer-rate Online Measurement (TOM) system

ABSTRACT

Shake flasks are widely used vessels for mammalian cell bioprocesses due to their efficiency and ease of scale-up during seed train preparation. However, noninvasive monitoring of respiratory activity in these vessels poses a challenge. In this study, we evaluated the effectiveness of a novel instrument, the Kuhner Transfer-rate Online Measurement (TOM) system, for real-time monitoring of respiratory activity in a CHO cell pool Fed-Batch process across two shake flask sizes. The results show that the TOM can effectively monitor process events and detect respiratory differences between flask sizes which is a key parameter that is rarely monitored during seed train preparation. Furthermore, the TOM demonstrated a strong correlation with increasing cell concentration, suggesting its potential as a soft sensor for biomass monitoring.

INTRODUCTION

The growth and metabolic function of mammalian cells are directly linked to their respiratory activity, which can be estimated by measuring changes in the concentration of O_2 and CO_2 inside a vessel [1, 2]. Recently, a new instrument called the Transfer-rate Online Measurement (TOM) system has been developed that can monitor respiratory activity in a similar way to the Respiration Activity Monitoring System (RAMOS) [3]. The TOM system operates in a closed system that simulates the aeration of an open vessel shake flask. Importantly this technology allows for continuous monitoring of shaken systems and thus can be used to determine the impact of routine process condition variations on respiratory activity. A lower $k_L a$ and OTR_{max} are typically observed with greater filling volumes in a shaken vessel [4]. During a fed-batch process, the filling volume gradually increases with each feed, resulting in a lower OTR_{max} . With an increase in specific productivity, the specific oxygen demand also increases [5]. This, increases the risk of the system becoming oxygen-limited before the end of the run. To address this issue, using a larger shake flask to reduce the total filling volume percentage and increase the OTR_{max} of the system is a viable solution. By comparing the OTR profiles across different shake flask sizes and filling volumes, we can efficiently plan these processes. In this study, we used the TOM to measure and compare the OTR and CTR profiles over a 14-day fed-batch process in 250mL and 1 L shake flasks.

MATERIALS AND METHODS

The study aimed to evaluate the growth and productivity of CHO stable pool cells expressing SARS-CoV-2 trimeric spike protein (Smt1) in shake flasks. The cells were cultivated in BalanCD CHO Growth A medium supplemented with MSX and fed with BalanCD CHO Feed 4 and glucose to maintain the required concentration. Seeded at 0.4 Mc/mL at 20% filling volumes, the cultures were shaken at 120 rpm in a Kuhner ISF1-X, and the temperature was shifted from 37°C to 32°C after three days of seeding. Induction was achieved with 4-Isopropylbenzenecarboxylate (cumate), concomitantly with the temperature shift. The cells growth and productivity were monitored by measuring cell density, viability, and metabolites (glucose, lactate, ammonia) at various time points, utilizing the previously reported methodology [6-7]. The online data were gathered every 1.5 hours using the TOM, which continuously measured the oxygen transfer rate (OTR) and carbon dioxide transfer rate (CTR).

Results

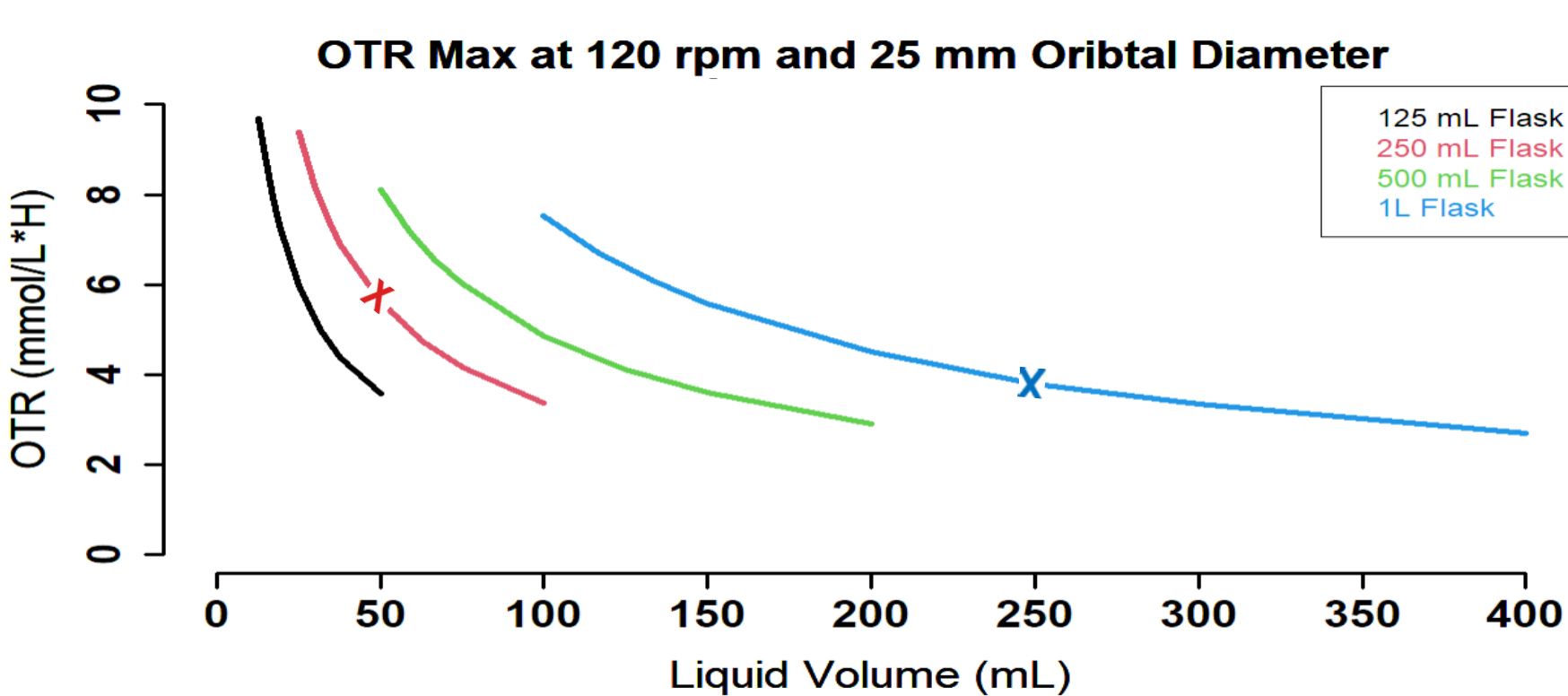


Figure 1. Relationship between OTR and filling volumes

Using the Kuhner tool for theoretical OTR calculation [8], the relationship between OTR and filling volume is graphed for various flask sizes at the same shaking rate and orbital diameter (Figure 1). Filling volumes between 10% and 40% were chosen as to give an accurate representation of experimentally acceptable liquid volumes. It can be discerned that the OTR of a larger flask at the same volume is higher but at the same % of filling volume, the OTR is equal or less [4]. This is important when we consider that the realized process is a fed-batch culture that increases in volume during every feeding event. Consideration must be taken such that peak OUR requirement does not surpass maximum OTR and thus creates an oxygen limiting environment. When noting table 1, we can observe that despite the change in flask size, the mean OTR/CTR during the growth phase is almost half as much as the mean OTR/CTR during the production phase. Interestingly, it is also noticeable that the mean OTR in the 1 L flasks is 1.24-fold larger when compared to the production phase OTR mean for the 250 mL flasks. A similar pattern (1.43-fold) holds for the CTR.

Table 1. Respiratory profiles summary.

	Growth Phase	Production Phase
250 mL OTR (mmol/L*H)	0.58	0.96
250 mL CTR (mmol/L*H)	0.37	0.76
250 mL TQ (Transfer Quotient = CTR/OTR)	0.64	0.79
1 L OTR (mmol/L*H)	0.54	1.19
1 L CTR (mmol/L*H)	0.42	1.09
1 L TQ (Transfer Quotient = CTR/OTR)	0.78	0.92

The viability of the cells in both the 250mL and 1 L flasks remained similar (<2%) from 0 to 14dpi, but the viable cell density (VCD) was found to be higher in the 1 L flask after around 7dpi (Figure 2). Furthermore, a comparable trend in the oxygen transfer rate (OTR) profile was observed between the two flask sizes, differing from 6 dpi onwards. (Figure 4), indicating that OTR may be a useful tool to compare the VCD profiles between shake flasks of different sizes. No strong variation was observed in the metabolic profile as seen in figure 3.

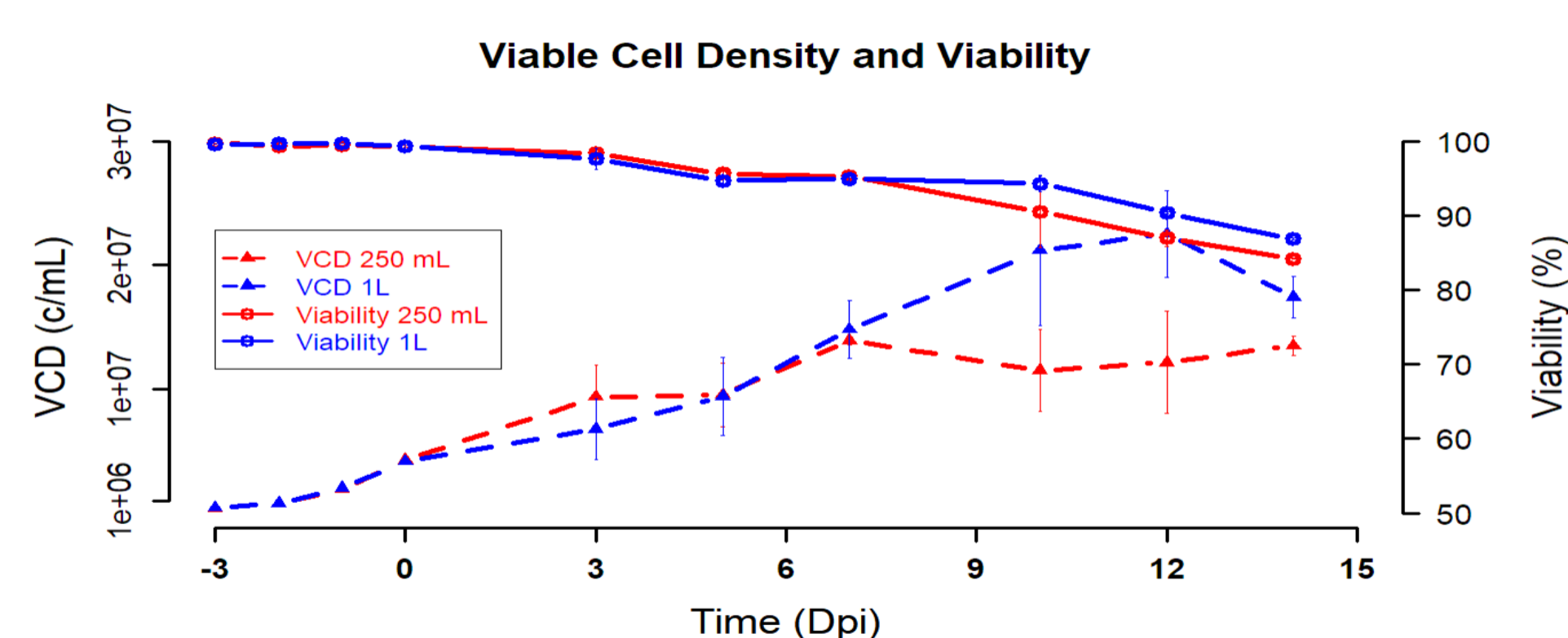


Figure 2. Cellular growth profile

Off-line measurements of Viable Cell Density (dashed line) and Viability (solid line) over the Fed-Batch process.

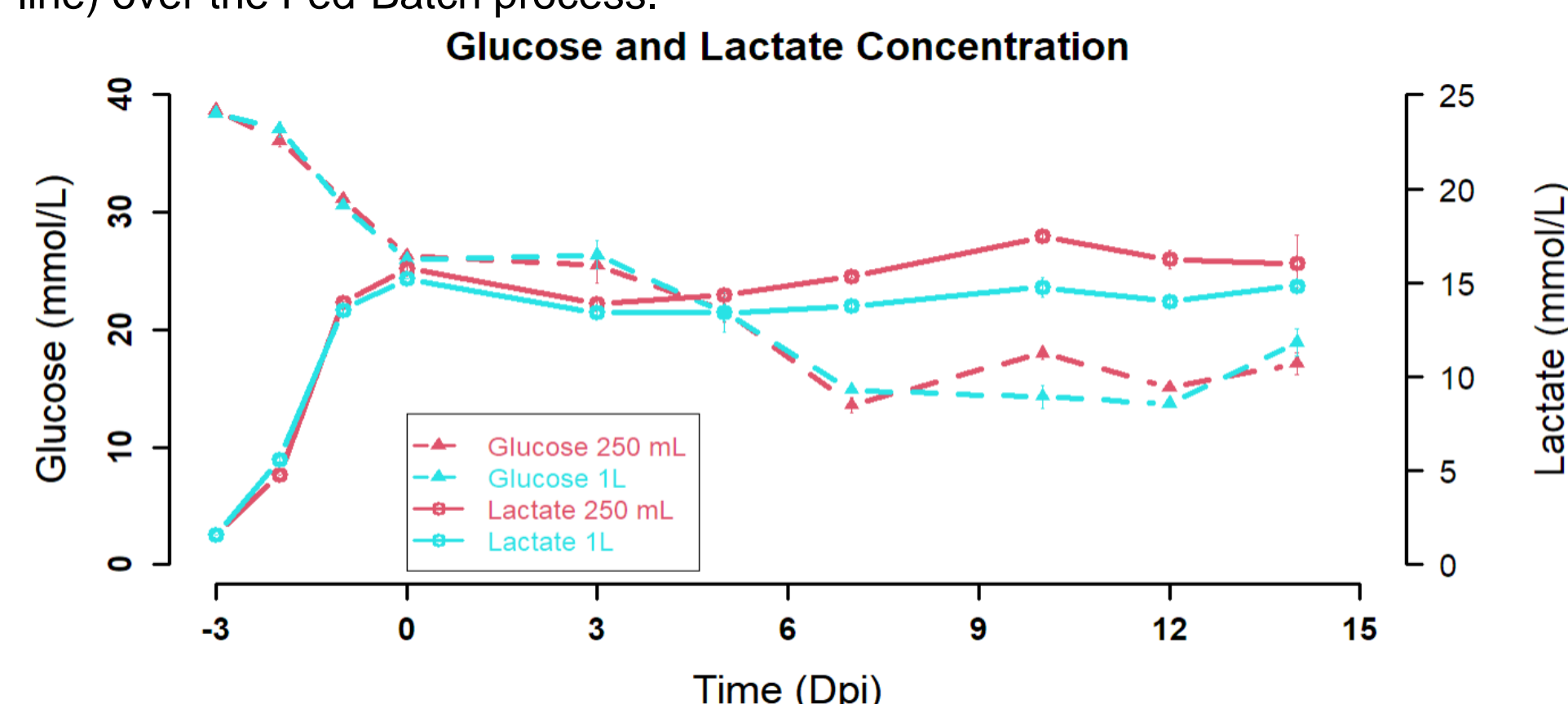


Figure 3. Metabolic (residual glucose and lactate) profile

Off-line measurements of glucose (dashed line) and lactate (solid line) over the Fed-Batch process.

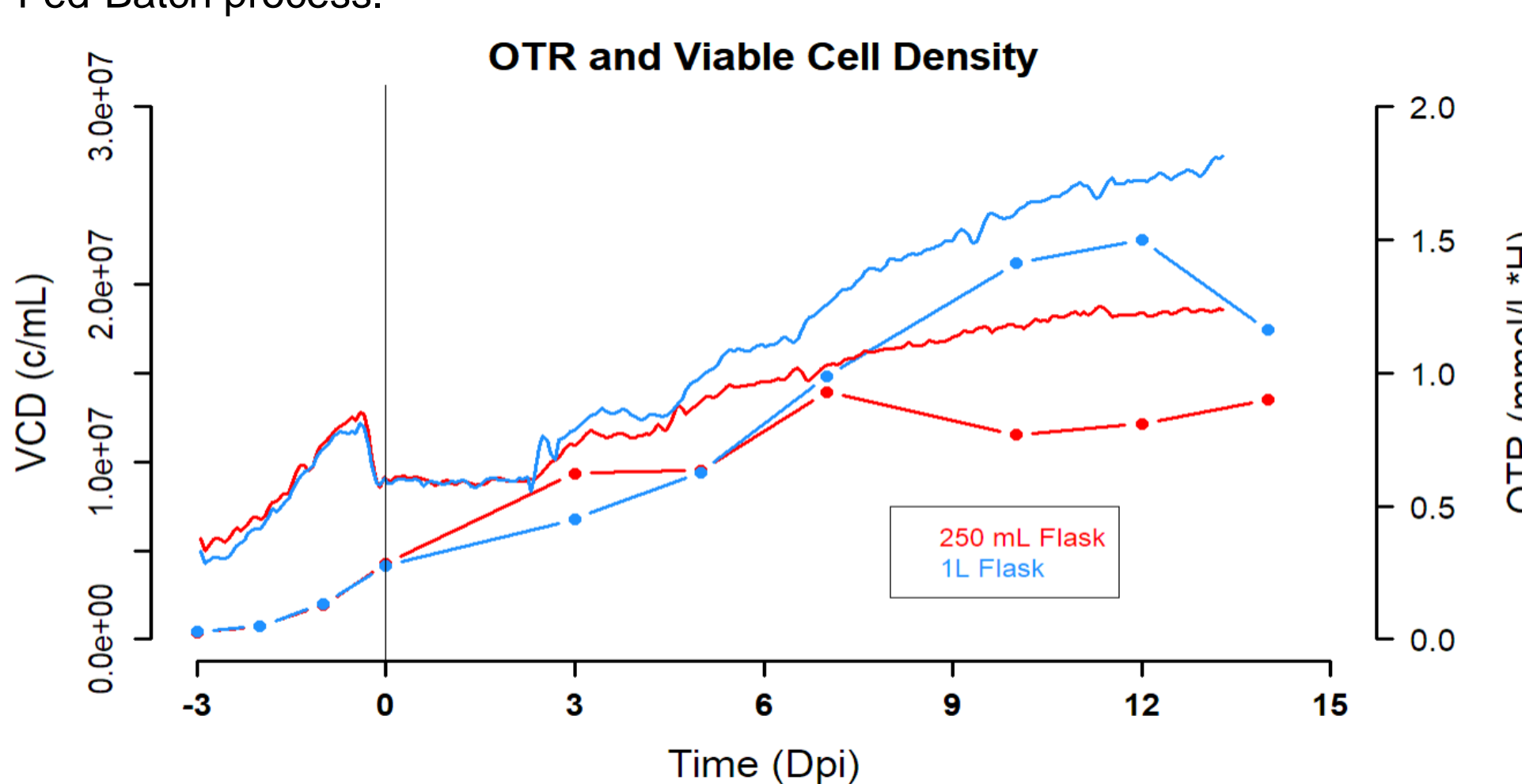


Figure 4. Overlay OTR and Cell Growth (VCD) data

Viable cell density and oxygen transfer rate profiles.

As the biomass increases, so will the demand for oxygen in the culture; consequently, the OTR should correlate with cell growth. It should also give indirect information about the metabolic demand of the cells in the culture. As it can be seen from figure 4, the sudden increase in cell concentration in the 1 L flasks is captured in the OTR trend in which a large increase in oxygen requirements are observed. Similarly, the plateau in cell concentration is also noted as a plateau in the oxygen requirements of the 250 mL flasks. It must be noted that theoretical OTR_{max} is not reached for both vessel sizes.

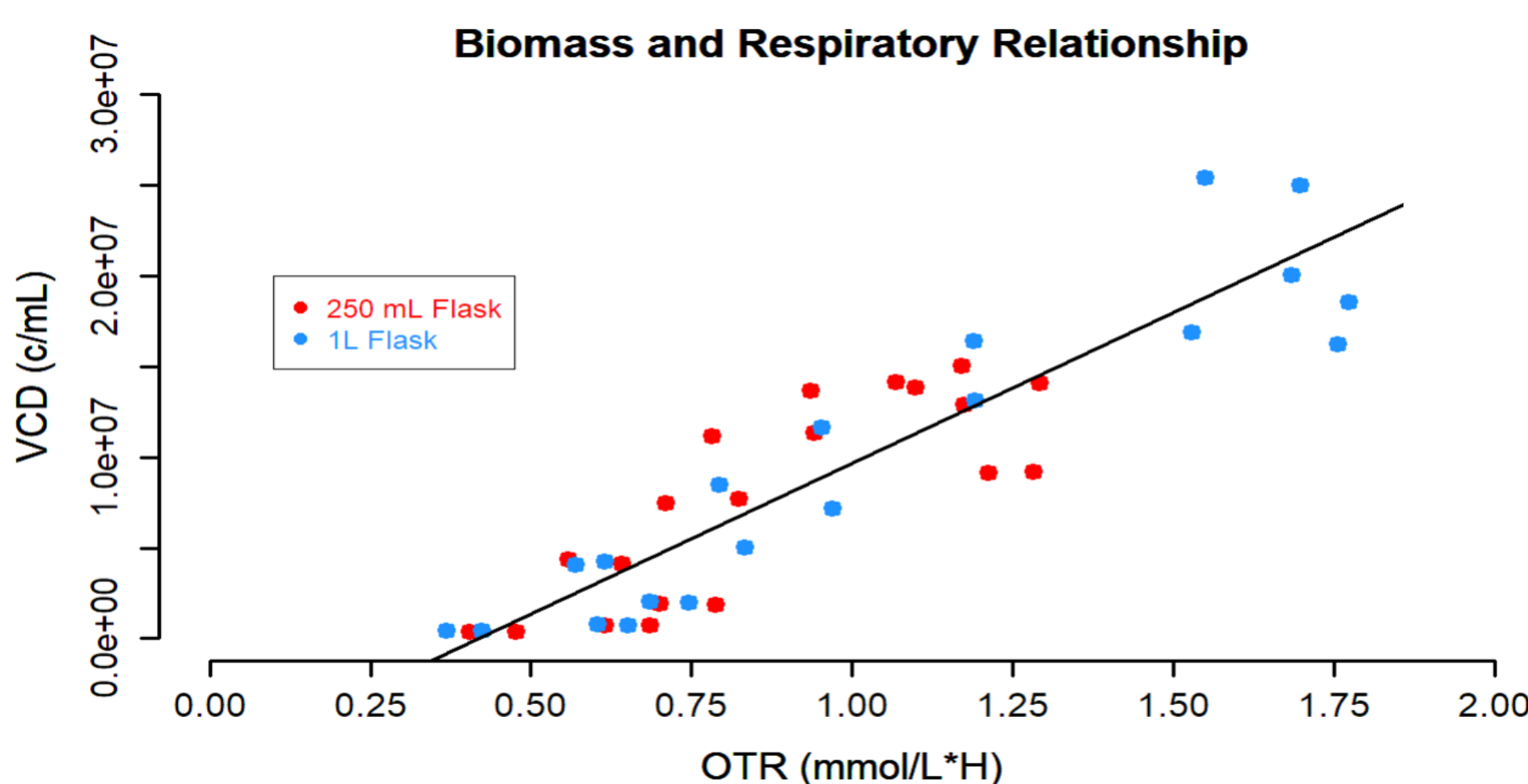


Figure 5. Scatter plot between VCD and average sampling day OTR

Given that a strong trend was observed in the OTR signal with respect to the cellular counts, a linear regression was carried out to determine how linear this relationship was. The average R^2 value is of 0.89. Interestingly, we can see that the cloud of points has a similar slope across both flask sizes indicating similar respiratory patterns.

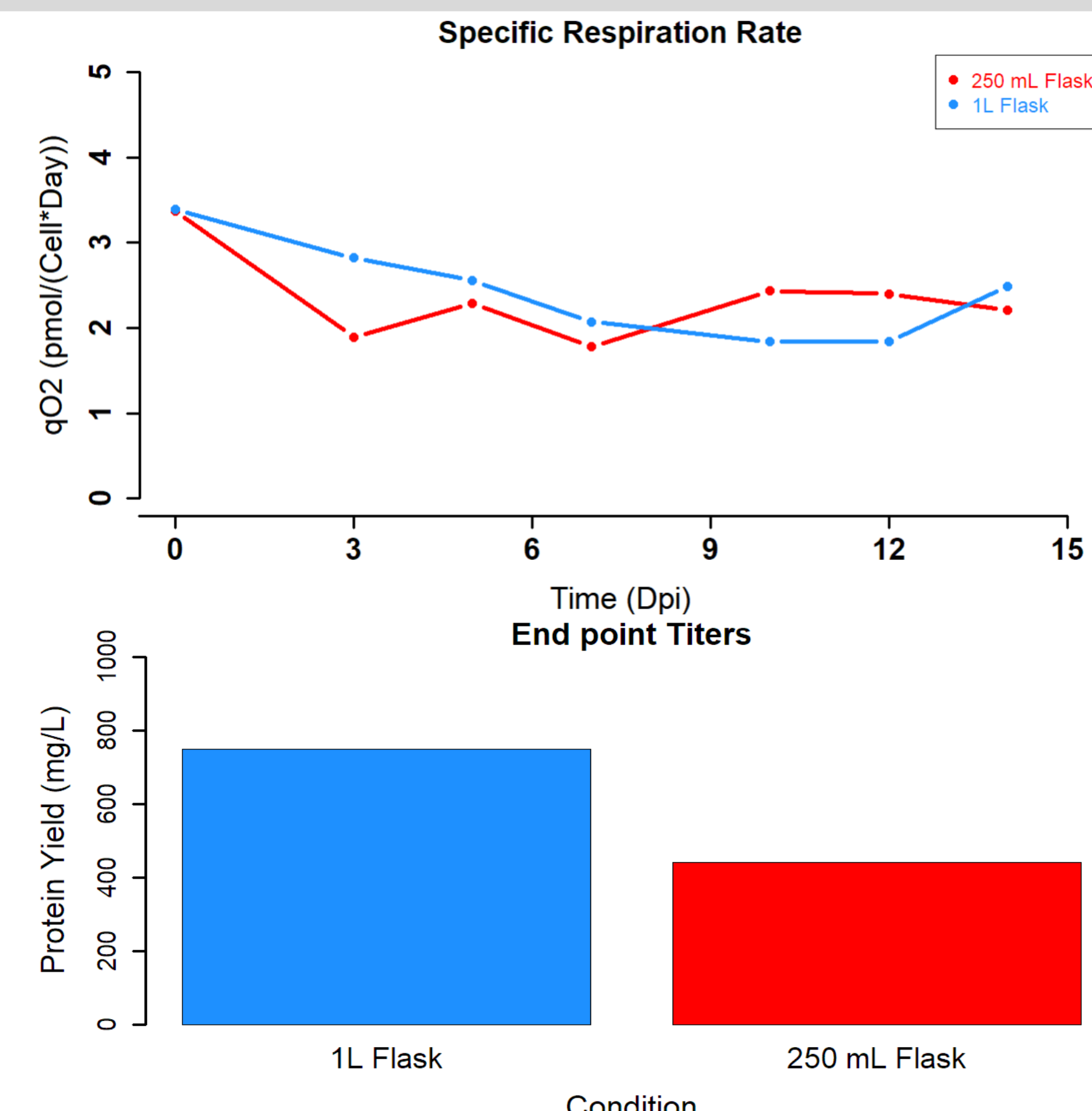


Figure 6. A) Specific Respiration Rate profile B) Endpoint titers.

The specific respiration rates ($qO_2 = OTR/VCD$) are plotted for each vessel size from 0 dpi to 14 dpi. Protein production is plotted at 14dpi.

The strong linear correlation (Figure 5) hints that specific respiration rates remained more or less constant across the culture run. As such, specific respiration rates were calculated. As it can be visualized (Figure 6 A), the specific respiration rates did not vary much after induction oscillating between 2-4 pmol/cell/day. However, mean respiration rates in the 1 L vessels were larger than in the 250 mL vessels (2.44 pmol/cell/day > 2.31 pmol/cell/day). Specific respiration rates (qO_2) are an important descriptor of a culture since it determines the individual oxygen consumption of each cell in a culture. qO_2 has been highly correlated with TCA activity and thus protein production [8]. Although qO_2 has been determined to be constant during the growth phase ($OUR = qO_2 * Biomass$), the relationship can vary during plateau/production phases of a cell culture, indicating that biomass alone cannot be responsible for changes in oxygen consumption [9]. Final titers show that the 1L flask produced more protein (Figure 6B). Although this could be because of higher viable cell densities. The specific protein production of the large flask was also higher indicating that the difference in biomass alone was not enough to explain the difference in final yield (3.88 pg/c/day > 3.19 pg/c/day). Since average specific oxygen consumption was also higher in the 1L flask, it could hint at a relationship between specific protein production and specific respiration rates.

CONCLUSION

We successfully implemented the TOM system into our CHO cell culture production platform at the NRC for a Fed-Batch process across two vessel sizes. The OTR and CTR data collected from the TOM align with the expected cell growth and production behavior that is typically observed for these cells; this includes the distinctive lag (-3 dpi), exponential growth (-2 - 0 dpi), plateau (6-12dpi), and deceleration phase (14 dpi) over a 17-day Fed-Batch process. Given the knowledge of how a standard Fed-Batch process is reflected on the OTR/CTR profiles, the TOM was then applied in the study of different vessel sizes to evaluate variations in growth, metabolic, respiratory profiles, and final titer. It was noted that the protein production in the 1 L vessels yielded higher protein concentration when compared 250 mL flasks which was mirrored by higher OTR in the 1 L flasks. Given the metabolic significance of oxygen consumption and the ability of gathering online measurements, the TOM may be utilized as a soft-sensor for biomass [9]. It must be noted that OTR_{max} is never reached for either vessel size and thus differences in growth profiles cannot be explained by oxygen limitations. However different vessel sizes at equal shaking and orbital diameters implies differing $k_L a$ values and differing dissolved oxygen tensions. These variations may impact cellular behavior which is then evidenced by the observed differences in growth and expression profiles.

The authors acknowledge the help of everyone at the NRC and Kuhner Shaker Inc. who made this study possible. This research received funding from the NRC's Pandemic Response Challenge Program.

References

- Anderlei, T., Zang, W., Pappaspyrou, M., & Büchs, J. (2004). Online respiration activity measurement (OTR, CTR, RQ) in shake flasks. *Biochemical Engineering Journal*, 17(3), 187-194.
- Anderlei, T., & Büchs, J. (2001). Device for sterile online measurement of the oxygen transfer rate in shaking flasks. *Biochemical Engineering Journal*, 7(2), 157-162.
- Kuhner TOM ONLINE MEASUREMENT. (n.d.). Retrieved April 27, 2021, from https://kuhner.com/en/products/data/Anwendungstechnologien_KuhnerTOM.php
- Doran, P.M. (2013). *Bioprocess engineering principles* (2nd ed., Ser. Engineering professional collection). Academic Press.
- Zalati, D., et al. A control strategy to investigate the relationship between specific productivity and high-mannose glycoforms in CHO cells. *Appl Microbiol Biotechnol*, 2016, 100(16), p. 7011-24.
- Stuble, M., Gervais, C., Lord-Dufour, S., Perret, S., L'Abbe D., Schrag, J., St-Laurent, G., Durocher, Y. (2021). Rapid, high-yield production of full-length SARS-CoV-2 spike ectodomain by transient gene expression in CHO cells. *Journal of Biotechnology*, 326, 21-27.
- Poullain, A., Perret, S., Malenfant, F., Mullick, A., Massie, B., Durocher, Y. (2017). Rapid protein production from stable CHO cell pools using plasmid vector and the cumate gene-switch. *Journal of Biotechnology*, 255, 16-27.
- Kuhner. (n.d.). Retrieved March 8, 2023, from https://kuhner.com/en/otr-calculator/index.php?fbclid=IwAR2ad5RBT8KpXQbe-gSdQpyFip7hYbdBaXpkiEua3CjQ7NdiBp-fY6ct_1c
- Reyes, S.J.; Durocher, Y.; Pham, P.L.; Henry, O. Modern Sensor Tools and Techniques for Monitoring, Controlling, and Improving Cell Culture Processes. *Processes* 2022, 10, 189. <https://doi.org/10.3390/pr10020189>